Author Manuscript

Author Manuscript

Author Manuscript

Author Manuscript

HHS Public Access

Author manuscript

Immunity. Author manuscript; available in PMC 2021 July 09.

Published in final edited form as:

Immunity. 2021 March 09; 54(3): 397–398. doi:10.1016/j.immuni.2021.02.005.

Essential functions of regulatory T cell TGF-β1 revealed by differential gene-targeting approaches

Emmanuel Stephen-Victor[1,2], **Ye Cui**[1,2], **Ziwei Wang**[1], **Mehdi Benamar**[1,2], **Louis-Marie Charbonnier**[1,2], **Talal A. Chatila**[1,2]

[1]Division of Immunology, Boston Children's Hospital, Boston, MA, 02115 USA.

[2]Department of Pediatrics, Harvard Medical School, Boston, MA, 02115 USA.

Responding to our recently published report (Turner et al., 2020), Velegraki *et al* (Velegraki et al., 2021) claimed that the Loxp elements around exon 6 of *Tgfb1* allele employed in our studies are predicted not to lead to deletion of the targeted exon but rather to its inversion. They further hypothesized that such an inversion of the targeted sequence would result in the eventual loss of chromosome 7, harboring the targeted *Tgfb1* allele, due to generation of an acentric and a dicentric chromosome stemming from asymmetrical chromosomal exchange between the sister chromatids. They further claim that such a phenomenon would lead to the apoptosis during cell cycle and eventually the depletion of regulatory T (Treg) cells, thus phenocopying *Foxp3* deficient mice. Accordingly, the phenotype of mice with Treg cell-specific *Tgfb1* exon 6 deletion would be the result of Treg cell depletion rather than their *Tgfb1* deficiency.

To investigate these claims, we analyzed the targeted genomic *Tgfb1* exon 6 region in sorted Treg cells isolated from *Foxp3*$^{\text{YFPcre}}$ *Tgfb1*$^{\text{Exon6Δ/Δ}}$ as compared to control *Foxp3*$^{\text{YFPcre}}$ mice, and also sequenced the pre-excision proximal and distal Loxp elements (Figure 1A). We employed PCR primers that bracketed a 1400 base pair (bp) region spanning across the floxed sequence (primers P1 and P2, Figure 1A), whose deletion would be predicted to give rise to a 350 bp sequence. Accordingly, we successfully amplified the predicted post-excision genomic product in the Treg cells of mutant *Foxp3*$^{\text{YFPcre}}$ *Tgfb1*$^{\text{Exon6Δ/Δ}}$ but not *Foxp3*$^{\text{YFPcre}}$ mice (Figure 1B, large arrow). Sequencing of this product clearly revealed the transition from an intron 5 sequence immediately 5' of the original position of the proximal Loxp element, continuing through a retained post-excision composite Loxp sequence, and leading into an intron 6 sequence 3' to the original distal Loxp sequence (Figure 1C). A correctly oriented DNA fragment corresponding to the sequence targeted for excision by the two Loxp elements was also amplified from the control Treg cells but was much reduced in the mutant Treg cells (Figure 1B, small arrow). No amplified sequences running in the reverse orientation were detected (data not shown). These results refute the claim that the targeted sequence is not deleted in *Foxp3*$^{\text{YFPCre}}$ *Tgfb1*$^{\text{Exon6Δ/Δ}}$ Treg cells. They also are in agreement with the results reported in the original report on the generation of the *Tgfb1* exon 6 floxed allele, which was successfully deleted by a *Lck* promoter driven Cre recombinase (Azhar et al., 2009). Extrapolating from our published results of real time PCR quantitation of exon 6 containing *Tgfb1* mRNA in *Foxp3*$^{\text{YFPcre}}$ *Tgfb1*$^{\text{Exon6Δ/Δ}}$ versus control *Foxp3*$^{\text{YFPcre}}$ Treg cells, we estimate the efficiency of the Cre-mediated *Tgfb1* exon 6 excision at about 90%. This estimate is also supported by a virtually identical decrease in

Author Manuscript Author Manuscript Author Manuscript Author Manuscript

secreted TGF-β1 protein production in anti-CD3+anti-CD28 mAb-activated mutant Treg cell cultures as measured by ELISA (Turner et al., 2020).

We next addressed the claim that the phenotype of *Foxp3*^{YFPcre} *Tgfb1*$^{Exon6\Delta/\Delta}$ mice relates to the depletion of Treg cells. Analysis of Treg cell frequencies and absolute numbers in different lymphoid tissues of *Foxp3*^{YFPcre} *Tgfb1*$^{Exon6\Delta/\Delta}$ versus *Foxp3*^{YFPcre} mice revealed no difference in the frequencies of Treg cells in peripheral and mesenteric lymph nodes (PLN and MLN) in the respective mice, whereas the absolute number of Treg cells were statistically significantly higher in the PLN of *Foxp3*^{YFPcre} *Tgfb1*$^{Exon6\Delta/\Delta}$ mice (Figure 1D, E). Whereas the spleens of *Foxp3*^{YFPcre} *Tgfb1*$^{Exon6\Delta/\Delta}$ mice exhibited reduced frequencies of Treg cells, their absolute numbers were similar to those found in the spleens of *Foxp3*^{YFPcre} mice (Figure 1F). Only in the blood were the frequencies and absolute numbers of Treg cells reduced by about 50% in *Foxp3*^{YFPcre} *Tgfb1*$^{Exon6\Delta/\Delta}$ mice, most likely reflective of dysregulated homing to lymphoid and inflamed somatic tissues (Figure 1G). Analysis of *Foxp3*^{YFPCre} *Tgfb1*$^{Exon6\Delta/+}$ mice heterozygous for the floxed allele revealed overall similar frequencies and numbers across the different tissues as those of *Foxp3*^{YFPCre} mice. Notably, analysis of splenic Treg cell apoptosis by Annexin V staining showed no statistically significant difference between *Foxp3*^{YFPcre}, *Foxp3*^{YFPcre} *Tgfb1*$^{Exon6\Delta/+}$ and *Foxp3*^{YFPcre} *Tgfb1*$^{Exon6\Delta/\Delta}$ mice (Figure 1H). Furthermore, we analyzed the mRNA expression of several genes along chromosome 7, including *Ffar2*, *Il4ra*, *Irf7* and *Relb*. Expression of these genes in the mutant Treg cells was either similar to or increased compared to WT Treg cells, arguing against the loss of chromosome 7 in the targeted Treg cells (Figure 1I). This conclusion is consistent with our previous demonstration in our publication that in heterozygous *Foxp3*$^{YFPcre/+}$ *Tgfb1*$^{Exon6fl/fl}$ female mice, the exon 6 deletant mutant Treg cells (*Foxp3*^{YFPcre} *Tgfb1*$^{Exon6\Delta/\Delta}$) had a similar fitness as their exon 6 sufficient (*Foxp3*$^{+}$ *Tgfb1*$^{Exon6fl/fl}$) Treg cell counterparts circulating in the same mice (Turner et al., 2020). The claim that transgenic TGF-β1 expression from the Rosa26 locus failed to rescue the *Foxp3*^{YFPcre} *Tgfb1*$^{Exon6\Delta/\Delta}$ excision phenotype cannot be evaluated as evidence of transgenic TGF-β1 expression, analysis of the tissue and cellular phenotypes and the outcome in terms of survival were all not reported, Overall, these results refute the claim the phenotypes of *Foxp3*^{YFPcre} *Tgfb1*$^{Exon6\Delta/+}$ and *Foxp3*^{YFPcre} *Tgfb1*$^{Exon6\Delta/\Delta}$ mice are due to Treg cell depletion, confirming instead that they arise specifically as a result of Treg cell-specific TGF-β1 deficiency

Both Velegraki *et al* (Velegraki et al., 2021) and Choi *et al* (Choi et al., 2021) present data that deletion of *Tgfb1* exon 2 in Treg cells does not give rise to autoimmune lymphoproliferation. We have previously hypothesized that deletion of proximal exons of *Tgfb1* may give rise to hypomorphic phenotypes due to the continued expression of active TGF-β1 from the distal exons 5-7 by means of alternative open reading frames. To validate our hypothesis, we recently evaluated mice with Treg cell specific exon3 deletion (*Foxp3*^{YFPcre} *Tgfb1*$^{Exon3\Delta/\Delta}$) (Jax Lab). Phenotypically, and similar to the exon 2 deletants reported by Velegraki *et al* (Velegraki et al., 2021) and Choi *et al* (Choi et al., 2021) the *Foxp3*^{YFPcre} *Tgfb1*$^{Exon3\Delta/\Delta}$ mice appeared healthy. Analysis of TGF-β1 production by ELISA revealed that whereas the production of secreted TGF-β1 (both inactive proprotein and mature active TGF-β1) was mostly abrogated in activated *Foxp3*^{YFPcre} *Tgfb1*$^{Exon6\Delta/\Delta}$ as compared to similarly treated *Foxp3*^{YFPcre} Treg cells, substantial residual TGF-β1

Author Manuscript Author Manuscript Author Manuscript Author Manuscript

production by *Foxp3*^{YFPcre} *Tgfb1*$^{Exon3\Delta/\Delta}$ Treg cells could still be detected (Figure 1J). Immunoblot analysis revealed that whereas exon 6 deletion decreased the expression of latency associated peptide (LAP) and mature TGF-β1 (both dimeric and monomeric forms), exon 3 deletion largely spared the latter (Figure 1K).

Notwithstanding their normal appearance, *Foxp3*^{YFPcre} *Tgfb1*$^{Exon3\Delta/\Delta}$ mice exhibited allergic dysregulation both at baseline and upon oral sensitization with chicken egg ovalbumin (OVA) as a model food allergen. This phenotype manifested despite these mice being on a C57BL/6 background, normally associated with reduced allergic response. Oral challenge of sensitized *Foxp3*^{YFPcre} *Tgfb1*$^{Exon3\Delta/\Delta}$ mice with OVA resulted in intense anaphylaxis as evidenced by the drop in their core body temperature (Figure 1L). Other stigmata of a severe food allergic response in the sensitized *Foxp3*^{YFPcre} *Tgfb1*$^{Exon3\Delta/\Delta}$ mice included elevated total and OVA-specific IgE responses, mast cell degranulation as evidenced by elevated serum concentrations of mast cell protease 1(MCPT1) and expansion of mast cell numbers in the small intestine as detected by flow cytometry ($Lin^{-}CD45^{+}cKit^{+}Fc\varepsilon R1^{+}IgE^{+}$) (Figures 1M-1O). Overall, the allergic dysregulation exhibited by mice with Treg cell-specific homozygous *Tgfb1* exon 3 deletion approximated that of mice with Treg cell-specific exon 6 haploinsufficiency or partially penetrant exon 6 deletion using a bacterial artificial chromosome encoded, *Foxp3* promoter driven Cre recombinase.

We have previously demonstrated that *Tgfb1* exon 6 haploinsufficiency in Treg cells gave rise to allergic dysregulation by a mechanism involving depletion of gut Treg cells expressing the retinoic acid receptor-related orphan receptor γt ($ROR\gamma t^{+}$). Consistent with these findings, analysis of food allergic *Foxp3*^{YFPcre} *Tgfb1*$^{Exon3\Delta/\Delta}$ mice revealed decreased frequencies of $ROR\gamma t^{+}$ Treg cells in the gut, with a reciprocal expansion of T helper-2 (Th2) cell-like reprogrammed Treg cells expressing elevated levels of the transcription factor GATA3 and the Th2 cell cytokine IL-4 (Figures 1P and 1Q). Altogether, these results confirm that Treg cell specific *Tgfb1* exon 3 deletion gives rise to a hypomorphic phenotype that approximates that observed with Tgfb1 exon 6 haploinsufficiency. The results of Choi *et al* (Choi et al., 2021) are consistent with an incomplete suppression of TGF-β1 production upon exon 2 deletion, suggesting that these mice may also manifest pronounced allergic dysregulation when tested using the appropriate experimental paradigms. Of note, *Tgfb1* exon 6 haploinsufficiency did not give rise to an exaggerated Th1 response, similar to what was revealed in a colitis model employed by Choi *et al* (data not shown).

In conclusion, the results reported herein reinforce and extended those reported earlier by us to indicate distinct phenotypes associated with Treg cell-specific TGF-β1 deficiency extending from allergic dysregulation to autoimmunity, the nature and magnitude of which is governed by the level of residual TGF-β1 production by Treg cells (Turner et al., 2020). These results warrant further investigations on the molecular regulation of *Tgfb1* expression in Treg cells and how it may contribute to disease.

Acknowledgments

This work was supported by NIH NIAID grants 5R01AI126915 and 5R01AI085090 (T.A.C.).

Author Manuscript Author Manuscript Author Manuscript Author Manuscript

References

Azhar M, Yin M, Bommireddy R, Duffy JJ, Yang J, Pawlowski SA, Boivin GP, Engle SJ, Sanford LP, Grisham C, et al. (2009). Generation of mice with a conditional allele for transforming growth factor beta 1 gene. Genesis 47, 423–431. [PubMed: 19415629]

Choi G, Kim B-S, Chang J-H, and Chung Y (2021). Defining the role of transforming growth factor b1 in Foxp3+ T regulatory Cells. Immunity 54, 393–394. [PubMed: 33691125]

Turner JA, Stephen-Victor E, Wang S, Rivas MN, Abdel-Gadir A, Harb H, Cui Y, Fanny M, Charbonnier LM, Fong JJH, et al. (2020). Regulatory T Cell-Derived TGF-beta1 Controls Multiple Checkpoints Governing Allergy and Autoimmunity. Immunity 53, 1202–1214 e1206. [PubMed: 33086036]

Velegraki M, Salem M, Ansaa-Addo EA, Wu BX, and Li Z (2021). Autocrine transforming growth factor b1 in regulatory T cell biology—gone but not missed. Immunity 54, 395–396. [PubMed: 33691126]

Author Manuscript Author Manuscript Author Manuscript Author Manuscript

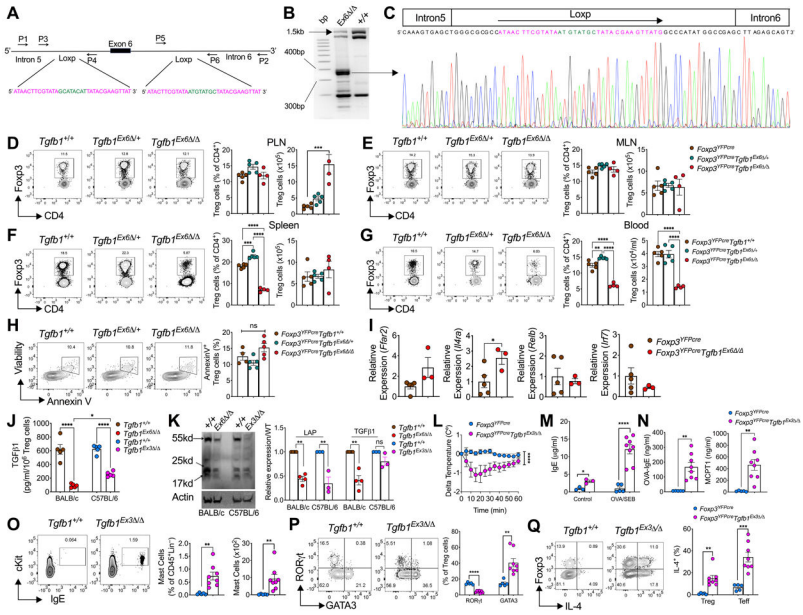

Figure 1. Differential impact of *Tgfb1* exon 6 versus exon 3 deletion in Treg cells.

(A). Schematic presentation of the floxed *Tgfb1* exon 6 locus, detailing the proximal and distal Loxp sequences and the positions of the primers used in Sanger sequencing studies. Primers P1 and P2 were used to sequence the entire locus, P3 and P4 for the proximal and P5 and P6 for the distal loxp sites. (B). Gel electrophoresis analysis of P1 and P2 PCR amplicons obtained using genomic DNA of $Foxp3^{YFPCre}Tgfb1^{Ex6\Delta/\Delta}$ and $Foxp3^{YFPCre}$ Treg cells. Long arrow indicates the position of 350bp post Cre excision PCR product, while the short arrow indicates the position of the unexcised full length sequence. (C). Sanger sequencing of the 350bp Cre excision PCR product shown in panel B detailing the position of introns 5 and 6 and the post excision retained Loxp sequence. (D). Representative flow cytometric plots, frequencies and numbers of Treg cells in peripheral lymph nodes (PLN) (D), mesenteric lymph nodes (MLN) (E), Spleen (F), and Blood (G) from $Foxp3^{YFPCre}$, $Foxp3^{YFPCre}Tgfb1^{Ex6\Delta/+}$, and $Foxp3^{YFPCre}Tgfb1^{Ex6\Delta/\Delta}$ mice. (H). Representative flow cytometric plots and frequencies of Annexin V^+ Treg cells from the spleens of the respective mouse strains. (I). Real time PCR analysis of relative mRNA expression of *Ffar2*, *Il4ra*, *Relb*, and *Irf7* in $Foxp3^{YFPCre}$ and $Foxp3^{YFPCre}Tgfb1^{Ex6\Delta/\Delta}$ Treg cells. (J). ELISA Quantification of TGFβ1 production by anti-CD3+anti-CD28 mAb +IL-2-activated Treg cells isolated from $Foxp3^{YFPCre}$ and $Foxp3^{YFPCre}Tgfb1^{Ex6\Delta/\Delta}$ mice (BALB/c background) and $Foxp3^{YFPCre}$ and $Foxp3^{YFPCre}Tgfb1^{Ex3\Delta/\Delta}$ mice (C57BL/6 background). (K). Immunoblot analysis of TGFβ1 in cell lysate of Treg cells from $Foxp3^{YFPCre}$ and $Foxp3^{YFPCre}Tgfb1^{Ex6\Delta/\Delta}$ (BLAB/c) *and* $Foxp3^{YFPCre}$ and $Foxp3^{YFPCre}Tgfb1^{Ex3\Delta/\Delta}$ (C57Bl/6) mice. Representative immunoblot, densitometric analysis of latent TGFβ1 and mature TGFβ1 expression in Treg cells. (L). Core body temperature drop following OVA challenge of OVA-SEB sensitized $Foxp3^{YFPCre}$ and $Foxp3^{YFPCre}Tgfb1^{Ex3\Delta/\Delta}$ mice. (M) Serum concentrations of IgE at baseline and post Ova challenge; OVA-specific IgE and MMCP-1 (N-P). Flow cytometric analysis and enumeration of c-Kit^+Fcε$RI^+$$IgE^+$ mast cells, RORγt^+ and $GATA3^+$ Treg cells and IL-4^+ Treg and Teff cells (P) in the in the small intestines (SI) of the mouse groups in (L). Results are representative of at least 3

Author Manuscript Author Manuscript Author Manuscript Author Manuscript

independent experiments. Each symbol represents an independent sample. Numbers in flow plots indicate percentages. Error bars indicate SEM. Statistical tests: Two-way ANOVA (L); One-way ANOVA (D, E, G, H) Student's t-test (I to K; and M to Q). *P<0.05, **P<0.01, ***P<0.001, ****P<0.0001.